Thermal degradation of conventional and nanoencapsulated azoxystrobin due to processing in water, spiked strawberry and incurred strawberry models.

Peiying Wang[1], Valérie Gravel[2], Vinicius Bueno[3], Juliana A. Galhardi[4], Subhasis Ghoshal[3], Kevin J. Wilkinson[4], Stéphane Bayen[1*]

[1]*Department of Food Science and Agricultural Chemistry, McGill University, Ste-Anne-de-Bellevue, QC, Canada, H9X 3V9*
[2] *Department of Plant Science, McGill University, Ste-Anne-de-Bellevue, QC, Canada, H9X 3V9*
[3] *Department of Civil Engineering, McGill University, Montréal, QC, Canada, H3A 0C3*
[4] *Department of Chemistry, Université de Montréal, Montréal, QC, Canada, H3A 0B8*

ACS Agric. Sci. Technol. 2022, 2, 5, 960–968; DOI: 10.1021/acsagscitech.2c00119

*Corresponding author current address and email:
Department of Food Science and Agricultural Chemistry
McGill University, 21111 Lakeshore, Ste-Anne-de-Bellevue
Quebec, Canada, H9X 3V9
Email: stephane.bayen@mcgill.ca

Abstract

Nanoecapsulated formulations of pesticides have been recently developed and some products are now marketed for specific applications in agriculture. Pesticide residues present in raw agricultural products can degrade or react during food processing steps. To date, the fate of nanopesticides during food processing has not been well described. In this study, the thermal degradation of azoxystrobin (AZOX) in conventional and nanoencapsulated (Allosperse® and $nSiO_2$) formulations was first assessed in water, spiked strawberry and incurred strawberry models. The thermal degradation followed first-order kinetics when heated at 100°C in the water model. The thermal degradation of AZOX in nanoformulations in strawberry models (18% AZOX decrease) was comparable or lower than in the conventional formulation (21%), possibly due to the nanocarriers protecting the active ingredient from hydrolytic degradation. Out of 32 thermal degradation products (TDPs), only two were detected in both the spiked water and strawberry models, indicating differences in the thermal degradation reactions for AZOX in these two models. Identical TDPs were detected for both conventional and nanoformulations for each specific model, except for the absence of one (TDP22) in the $nSiO_2$ formulations. The nanoencapsulation of AZOX did not result in new TDPs in any of the matrices. Only six of the TDPs detected in water, four in spiked strawberries and two in incurred strawberries have been previously reported in environmental studies on the metabolism of AZOX. Based on the observed TDPs, AZOX thermal degradation pathways include ether cleavage, hydrolysis, demethylation and decarboxylation. Overall, although nanocarriers have no impact on the degradation product types, nanocarriers had a slight but significant impact on the degradation rate of pesticide active ingredient.

Keywords: Strawberry; Thermal degradation; Azoxystrobin; Non-target analysis; Nanoencapsulated pesticide

1. Introduction

Food processing can induce changes in the pesticide residue profiles in food through hydrolysis, volatilization, dissolution, metabolism, oxidation, and thermal degradation[1]. While most thermal degradation studies have reported changes in the levels of the parent pesticides, there is often little information on the newly formed degradation or transformation products. Degradation products could be comparable or even more toxic as compared to the parent compounds[2]. The formation of significant amounts of toxic degradation products or metabolites may then require their surveillance together with the parent pesticide compound, as illustrated by 3-hydroxy-carbofuran, a metabolite of carbofuran[3]. To address concerns about pesticide degradation products, the *Codex Alimentarius*[4], for example, has recommended that the fate of pesticides residues during processing should be investigated in order to identify the possible breakdown or transformation products.

Recently, nanoencapsulation has been introduced as a technique to increase the efficacy of pesticides and reduce the use of the active ingredients (AI). Pesticides applied as nanoformulations may behave differently in agri-food systems as compared to conventional formulations. In particular, nanocarriers are expected to improve the stability of the pesticide AI. For example, an improved thermal stability was observed for isoprocard, carbamate and chlorpyrifos, when encapsulated into zinc layered hydroxide modified with sodium dodecyl sulphate (ZLH-SES-PRO) nanocarriers[5].

Strawberry production can be significantly impacted by fungi, which can influence the culture yields and the quality of strawberries[6]. Fungicides are effective for preventing leather rot and powdery mildew of strawberry plants, both diseases responsible for up to 30% loss of the fruits [7,8]. The extensive use of pesticides is however reflected by a relatively frequent detection of

pesticide residues in strawberries in the market[9], representing some possible hazards to human health and the environment.

Azoxystrobin (AZOX) currently has a key position in the global fungicide market (e.g., strawberry cultivation) because of its highly efficient and broad-spectrum character[10]. To comply with food safety regulations in Canada, AZOX residues in strawberries should not exceed a maximum residue limit (MRL) of 10 mg/kg[11]. Metabolism and degradation of AZOX under field conditions have been reported applied for both conventional and nanoencapsulated formulations[12,13]. In particular, a controlled strawberry field experiment was performed over 2 growing seasons in order to compare AZOX metabolites applied as both nanoencapsulated and conventional formulations[13]. In addition to being consumed as fresh fruits (including in "pick your own" operations), strawberries are commonly processed as an ingredient in the preparation of value-added commodities such as jams. Such processing activities contribute to minimize post-harvest losses and make strawberry culture more profitable[14]. However, no data have been reported to date on the thermal degradation kinetics and the identity TDPs of AZOX during thermal processing of fruits such as strawberries.

The reduction of pesticide levels in food is influenced by parameters such as temperature and time, the type of food matrices and the structure of the pesticides[15]. The stability of AZOX during thermal processing was investigated in several food matrixes, but not in fruits such as strawberries. For example, an 11-92% decrease was observed for the AZOX level in peanuts after boiling for 30 min[16]. Aguilera et al.[17] reported that heating for 30 min did not reduce the concentration of AZOX in zucchinis, when considering water loss during cooking. Overall, depending on the cooking methods, both apparent decreases and increases in the AZOX concentrations (-92% to +60%) have been reported after heating[16-24]. To date, the fate of

nanoencapsulated AZOX during thermal processing has not been reported. In this context, it appears essential to identify TDPs for both conventional and nanoencapsulated AZOX to produce comprehensive risk assessments.

The aim of this study was to investigate the thermal degradation kinetic and TDPs of AZOX in conventional and nanoencapsulated pesticide formulations, using both targeted and non-targeted analysis. LC coupled with high-resolution mass spectrometry (HRMS) has emerged as a powerful tool for targeted and non-targeted investigations of degradation products. Targeted analysis is often applied to quantify specific degradation products, while non-targeted analysis investigates degradation product profiles and identifies unknown or unexpected compounds in the samples[25,26]. The use of spiked samples is generally recognized as inappropriate to evaluate the stability of pesticides during processing[27]. This study was therefore performed on incurred strawberries, but spiked water and strawberry models were also included for comparison. More specifically, this study aimed at identifying the thermal degradation/transformation products and compared the degradation kinetics and breakdown or reactions products of AZOX generated in these three models. Results were discussed in terms of thermal degradation pathways for AZOX. Ultimately, this study aims at determining specificities in the fate and behavior of nanoencapsulated pesticides.

2. Material and methods

2.1 Chemicals and reagents

Azoxystrobin (AZOX, CAS#131860-33-8) was purchased as a pure standard (≥98%) from Sigma-Aldrich (St. Louis, MO, USA). The deuterated analogue AZOX-d_4 (internal standard) and azoxystrobin free acid (R234886, AzFA, known degradation product of AZOX) were purchased from Toronto Research Chemicals (North York, ON, Canada). HPLC grade solvents (water,

acetonitrile (ACN), and methanol), anhydrous magnesium sulphate, sodium acetate, LC/MS grade formic acid and ammonium acetate (NH_4Ac) were obtained from Fisher Scientific (Pittsburgh, PA, USA). Primary Secondary Amine (PSA) salts used to clean up the poler interference were purchased from Agilent (Santa Clara, CA, USA). Allosperse® is a polyacrylic acid polymeric nanoparticle used as a nanocarrier for pesticides, including AZOX. Allosperse®-AZOX was prepared and supplied by Vive Crop Protection Inc. (Mississauga, Canada). The synthesis of porous hollow silica nanoparticles ($nSiO_2$) and their loading with AZOX was reported in Bueno & Ghoshal[28] and Bueno et al.[29], respectively. Stock solutions (100 mg/L) of the standards were prepared in methanol for further dilution to prepare spiked standards.

2.2 Field (incurred) strawberry samples

A controlled field experiment was carried at the Macdonald Campus of McGill University, Sainte-Anne-de-Bellevue, QC, Canada. Strawberry plants (*Fragaria* × *ananassa* Duch. "Seascape"), were cultivated under field conditions (n = 5) and exposed to different treatments (Table S1): (1) control; (2) Conventional; (3) Allosperse®; (4) $nSiO_2$. Briefly, strawberry bare root plants (Pépinière Lareault, Canada) were transplanted in the first week of June 2019. Plants were treated twice (total 7.6 mg active ingredient / pot, 15 and 30 days after transplanting) using a drench application for each of the pesticide formulations. Further details on the field experiment, plant phenology and pesticide accumulation have been described in Galhardi et al.[13] Fruits were collected and homogenized in a stainless-steel blender. All processed samples were stored at -80°C until analysis. AZOX in incurred samples were quantified in our previous study and ranged from 0.2 – 6.21 µg/kg fresh strawberry[13].

2.3 Spiked water and strawberries

The degradation of AZOX in the various formulations (conventional, Allosperse®, and $nSiO_2$) was first studied in a spiked HPLC water model (100 µg/L; pH=8). Aliquots (1 mL) were transferred into 2 mL amber glass vials for five different processing times. Samples were placed in a water bath in a floating rack to keep the cap above the water surface. Samples were heated 100°C for 0 min (t0), 30 min (t30), 60 min (t60), 120 min (t120), and 240 min (t240). After heating, the vials were cooled down rapidly in cold water. Heated water samples (t240, n=6) were used for the identification of the TDPs for the spiked HPLC water (10 mg/L of the different AZOX formulations to detect as many degradation products as possible, especially those with relatively low concentrations).

Control strawberries from the field were spiked with AZOX in the three formulations at two levels (1 mg/kg and 10 µg/kg; n=3 for each formulation). The high spiking level (1 mg/kg) was used for the comparison with the spiked water (1 mg/L). The low spiking level (10 µg/kg) was comparable with concentrations measured in the harvested strawberries (incurred, around 10 µg/kg) in the field trial[13]. Aliquots (5 g) of each of the above spiked strawberry samples were transferred to 20-mL glass vials and were placed in a water bath as described above for water.

2.4 Extraction of the pesticides and their thermal degradation products

For the strawberry, AZOX extraction was adapted from a method based on the original QuEChERS approach[30] and validated for the nanoencapsulated formulations[31]. Fresh fruits were homogenized in a stainless-steel blender (Waring, USA). 2 g of homogenized strawberry sample was weighed in a 15 mL plastic centrifuge tube and spiked with AZOX-d_4 (40 µg/kg). Four mL of 1% acetic acid in acetonitrile, 0.8 g of magnesium sulphate and 0.2 g of sodium acetate were added.

Samples were vortexed for 15 minutes, and then centrifuged at 2240 × g (5 min, 20°C). One mL of the supernatant was transferred to centrifuge tubes containing 50 mg PSA and 150 mg of $MgSO_4$. Solutions were then vortexed for 1 min, and finally centrifuged (2240 × g, 5 min, 20°C). For water samples, each aliquot was filtered (0.22 μm PTFE filter, Chrom4; Thuringen, Germany) into HPLC vials for LC/MS analysis. Prior to LC-MS analysis, water samples were spiked with internal standards: 40 μg/L of AZOX-d_4.

2.5 Liquid chromatography-electrospray ionization mass spectrometry (LC-ESI-MS) analysis

All samples were filtered through a 0.22 μm polytetrafluoroethylene filter (Chrom4; Thuringen, Germany) and were analyzed on an Agilent 1290 Infinity II liquid chromatograph (LC) coupled to a 6545 QTOF mass spectrometer (Agilent Technologies, Santa Clara, USA), operating in both positive and negative electrospray ionization modes (2 consecutive analyses). The LC separation was conducted on a Poroshell 120 phenyl hexyl column (Agilent Technologies; 2.7 μm × 3.0 mm × 100 mm) fitted with a Poroshell 120 EC-C18 (2.7 μm × 3.0 mm × 5 mm) guard column. For both positive and negative mode, elution was performed in gradient mode (0.4 mL min^{-1}) using A=water (0.1% formic acid and 5 mM NH_4Ac) and B=ACN:methanol (1:1, v/v; 0.1% formic acid and 5 mM NH_4Ac) (0 min: 70% A; 0-3 min: B increased from 30 to 100%; 3-6 min: 100% B; 6-8 min: B decreased from 100% to 30%). The injection volume was 10 μL and the column temperature was maintained at 30°C. Nitrogen was used as the drying gas (110°C, 12 L min^{-1}). The fragmentor voltage was 110 V and MS data was acquired in the 50-750 *m/z* range in full scan mode. Azoxystrobin TDPs were subsequently identified in the targeted MS/MS mode (optimal collision energy of 20 V). Reference ions (*m/z* at 121.0508 and 922.0098 in the positive

electrospray ionization mode (ESI+); 112.9856 and 1033.9881 for the negative mode (ESI-)) were used for automatic mass recalibration of each acquired spectrum.

2.6 Degradation kinetics of azoxystrobin

The first-order degradation model (Eq. 1) is a common model for the degradation of chemical residues in food[32]:

$$ln[C] = ln[C_0]-k\times t \quad \text{(Equation 1)}$$

where k is the first-order degradation rate constant (slope of the linear fit); C_0 is the initial concentration; C is the concentration after a heating time t. The model was considered acceptable when p values for the data sets were <0.05 in regression statistics analysis using Microsoft Excel (Microsoft Corporation, USA).

2.7 Data treatment

2.7.1 Quantification for degradation percentage

For the quantitative analysis of AZOX, data treatment was conducted using Agilent MassHunter Quantitative Analysis (Agilent Technologies, USA). Ions at 404.1247 and 372.0971 *m/z* were selected as the quantifier and qualifier ions for AZOX, respectively, and were extracted from the full scan data (extraction mass window ±10 ppm). The relative response of AZOX vs. AZOX-d4 was used for quantification[31]. The thermal degradation percentages were calculated as the ratios of the AZOX concentrations after and before heating.

2.7.2 Identification of the thermal degradation products (TDPs)

First, chromatograms were aligned using the Agilent Masshunter Profinder (Agilent Technologies), using tolerance for retention times (RT) of 0.15 min and mass differences of 10 ppm. Extracted molecular features in heated and unheated samples were compared using the Agilent Masshunter Profiler Professional software (Agilent Technologies) to obtain a list of tentative degradation/transformation compounds. A library of AZOX metabolites and degradation products was prepared using the Agilent Masshunter PCDL software (Agilent Technologies), based on formulae reported in the literature[33,34]. This library was used to screen the LCMS data for possible TDPs of AZOX. The MS/MS spectra of those TDPs were manually compared with spectra from the literature to increase confidence in the identification. The identity of AZOX free acid, as a major degradation product of AZOX, was further confirmed based on matching signals (RT=3.491 min for ion at 372.0971 *m/z*) with the pure reference standard.

2.8 Statistical analysis

Analysis of variance (ANOVA) using SPSS Statistics Software 27 (IBM, USA) was used to identify differences among results obtained for different pesticide formulations, by applying a confidence range of 95% (α=0.05, n=3). The results reported for strawberries were based on triplicate extractions (3 different samples for each treatment). Significant differences ($p \leq 0.05$) between average responses were evaluated using a Tukey's multiple-comparisons test.

3. Results and Discussion

3.1 Thermal degradation kinetic of azoxystrobin in different formulations

Thermal degradation kinetics of AZOX in different formulations (conventional, Allosperse®, $nSiO_2$) were first compared to that in water heated at 100°C. AZOX concentration decreased with time for all formulations, and all degradation kinetics followed a first-order model (Figure 1 & Table 1; $R>0.9876$, $P<0.05$). Hydrolysis is expected to be the main degradation mechanism at pH 8[35]. The first-order degradation rate constant (k), determined from the slope (absolute value) of the linear fit ranged from 0.0026 ± 0.0002 min^{-1} for the conventional formulation, to 0.0028 ± 0.0002 min^{-1} for AZOX encapsulated in $nSiO_2$, and to 0.002 ± 0.0002 min^{-1} for AZOX encapsulated in Allosperse®. In the equation, the slope for the Allosperse® (0.002) was significantly lower than that of the conventional pesticide (0.0026) or $nSiO_2$ (0.0028). In other words, AZOX in the Allosperse® formulation appeared to be more stable than the other formulations in water (100 µg/L). As the kinetics were slightly (but significantly) slower in the presence of Allosperse, the polymer nanocarrier is thought to protect the AZOX from thermal degradation.

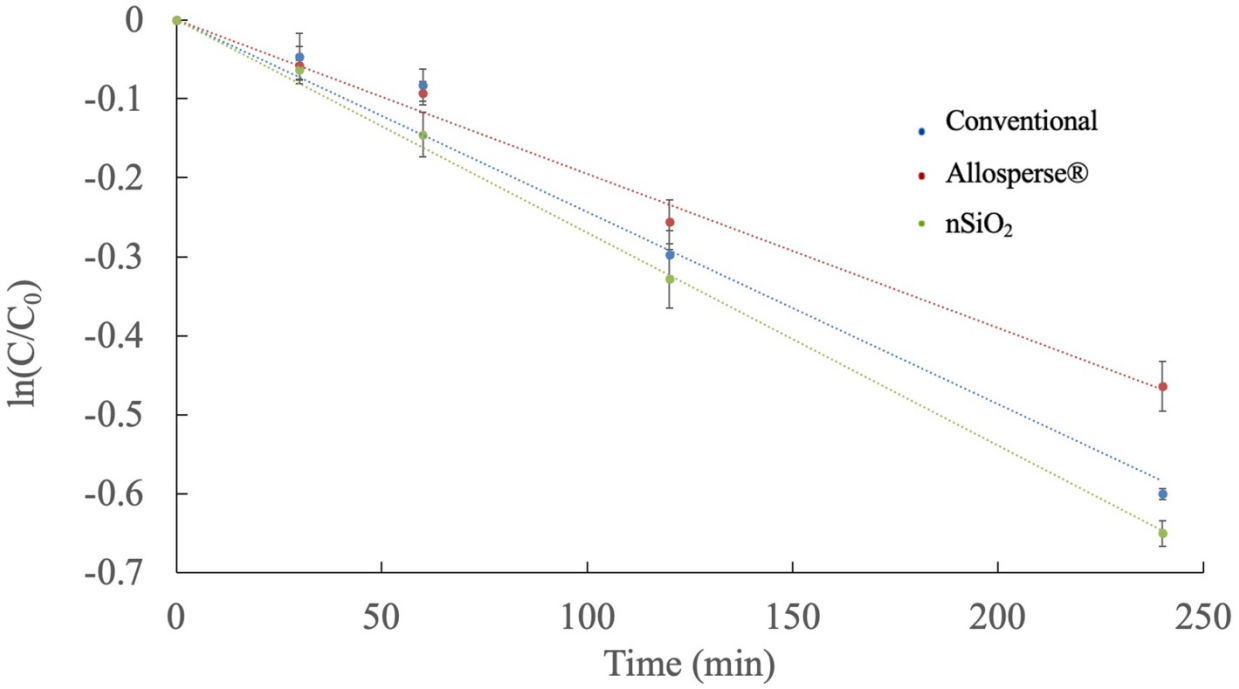

Figure 1 Ln(C/C_0) as a function of time (See Eq. (1)) for three formulations of azoxystrobin (conventional, Allosperse®, and $nSiO_2$) at 100°C in water (spiked with 100 µg/L). Regression line corresponds to a linear fit. The confidence level is 95% (n=3).

Table 1 Kinetics parameters of azoxystrobin thermal degradation at 100°C in water model.

	Conventional	Allosperse®	$nSiO_2$
First-order regression equation[a]	Y = -0.0026t + 0.0286	Y = -0.002t + 0.0035	Y = -0.0028t + 0.0107
r^2	0.9876	0.9926	0.9988
Rate constant (k, min^{-1})	0.00244 - 0.00287	0.0018 - 0.00227	0.00264 - 0.00292
p	3.5E-12	1.91E-11	1.12E-13

[a] Y = In C/C_0 C: concentration of azoxystrobin C_0: initial concentration of azoxystrobin; t = time

3.2 Degradation of azoxystrobin in different matrices

As the thermal degradation experiments were conducted in capped glass vials, concentration decrease of AZOX was estimated to be mostly attributed to thermal degradation, and not to volatilization (AZOX is poorly volatile). The thermal degradation percentages after 4 hours of heating of AZOX were significantly different for the formulations in water (100 µg/L and 1000 µg/L), spiked strawberries (10 µg/kg) and incurred strawberries (around 10 µg/kg) as shown in Figure 2. The thermal degradation percentages of AZOX in the incurred strawberries ranged from 16.0 ± 2.0% for the conventional formulation, to 14.0 ± 2.0% for AZOX encapsulated in Allosperse®, and 11.0 ± 2.0% for AZOX encapsulated in $nSiO_2$. For the spiked and incurred strawberries, thermal degradation percentages of AZOX in the nanoformulations were comparable or lower than for the conventional formulation. Nanocarriers may reduce the thermal degradation of AZOX, as observed in the strawberry models. As the release of AZOX from $nSiO_2$ has been shown to be controlled and prolonged over days under controlled conditions[29], the nanocarrier is anticipated to reduce interactions between the matrixes and AIs. The capacity to prevent the degradation of the loaded pesticide AI is often highlighted as one of the key features of nanoencapsulation for pesticide applications[36]. In the present test, nanoencapsulation had no consistent impact, as a range of effects were observed depending on the type of nanocarrier, the initial pesticide concentration and the matrices. Therefore, there are possibility of nanoencapsulation to increase the exposure of pesticides to human by increasing pesticide thermal stability.

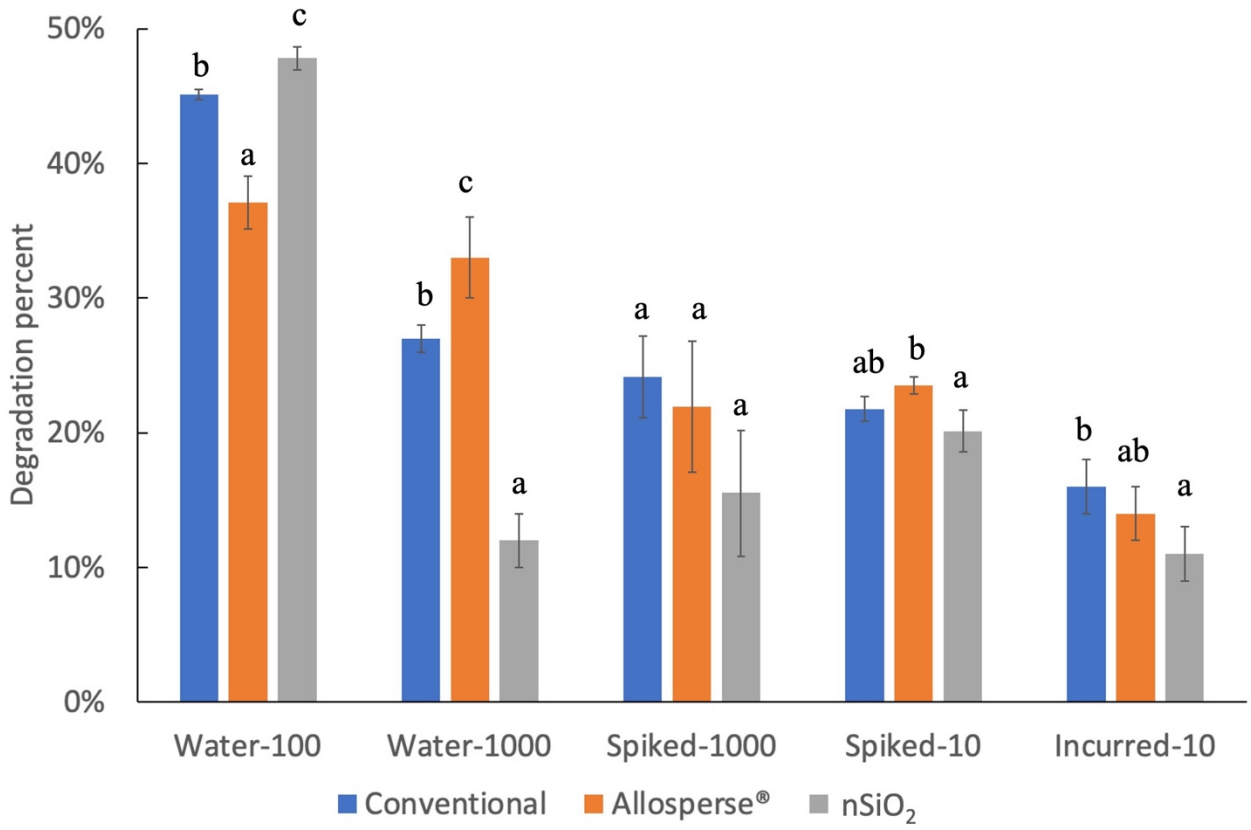

Figure 2 The degradation rate of the azoxystrobin (conventional, Allosperse®, and $nSiO_2$) at 100℃ in the water (100 µg/kg and 1000 µg/kg), spiked (1000 µg/kg and 10 µg/kg) and incurred (around 10µg/kg) strawberry models after 4 hours of heating (n=3). For each model separately, statistically significant differences between the different formulations are represented by different letters ($p<0.05$).

3.3 Identification of thermal degradation products of azoxystrobin

Compounds that may be considered as possible TDPs of AZOX in the spiked water, spiked strawberry and incurred strawberry models are listed in Table 2. Compounds present in both the control heated samples (matrices without pesticide formulations) and unheated samples were eliminated from the list. In heated water and strawberries, molecular features of interest were investigated in both ESI+ and ESI- modes. Although *Codex Alimentarius* recommends

investigating the breakdown or reaction products of pesticides generated by processing[4], there are no specific guidelines for the detection of TDPs of pesticides in food. Some TDPs detected in this study could not be detected in both ESI+ and ESI- modes. Therefore, both positive and negative ESI modes should be included the method development of pesticide TDPs to detect as many TDPs as possible. Some degradation or transformation products of AZOX in the environment (water, sediments, plants and soils) have been reported in the literature[33,34]. All of these AZOX metabolites were included in the PCDL library (Table S4). After the targeted scan, some molecular features suspected to be TDPs could be matched with specific reported compounds based on the ion *m/z* from the library (Table 3).

Table 2 Possible thermal degradation products of azoxystrobin identified in ESI+ or ESI- modes in spiked water, spiked strawberry and incurred strawberry models (100°C; 4 hours). ND: not detected.

Compound ID	Mass	*m/z*	RT	ESI[b] +/-	Peak Area[c]	Model		
						Spiked water	Spiked strawberries	Incurred strawberries
TDP 1	208.0731	209.0806	2.906	+	349239	ND	√	ND
TDP 2	213.0538	214.0617	2.440	+	2983	√	√	ND
TDP 3	218.0679	219.0759	2.617	+	163163	ND	√	ND
TDP 4	222.0527	221.0451	2.620	-	145253	ND	√	ND
TDP 5	228.0900	229.0970	3.423	+	24395	ND	√	ND
TDP 6	302.0903	303.0972	2.712	+	28005	√	√	ND
TDP 7	303.1010	304.1078/302.0931	3.619	+/-[d]	241256	√	ND	ND
TDP 8	317.0798	318.0867	3.908	+	143804	√	ND	ND
TDP 9	321.1106	322.1172/320.1032	3.717	+/-[d]	68062	√	ND	ND
TDP 10	325.0824	326.0892	3.622	+	35140	√	ND	ND
TDP 11	329.0802	330.0867/328.0729	3.944	+/-[d]	202201	√	ND	ND
TDP 12	347.0909	348.0973	3.509	+	123076	√	ND	ND
TDP 13	351.0615	352.0683	3.937	+	94766	√	ND	ND
TDP 14	361.0700	362.0760	2.955	+	19240	√	ND	ND
TDP 15	361.1073	362.1141	3.783	+	57327	√	ND	ND
TDP 16	361.1720	362.1620	3.576	+	33728	√	ND	ND

Compound ID	Mass	*m/z*	RT	ESI[b] +/-	Peak Area[c]	Model		
						Spiked water	Spiked strawberries	Incurred strawberries
TDP 17	369.0722	370.0790	3.498	+	47827	√	ND	ND
TDP 18	375.1328	376.1391	3.922	+	16945	√	ND	ND
TDP 19	389.1012	390.1081/320.1032	3.527	+/-[d]	220640	√	ND	ND
TDP 20	393.0066	394.1385	3.271	+	50615	ND	√	ND
TDP 21	405.1435	406.1503	3.502	+	10524	√	ND	ND
TDP 22[a]	407.1118	408.1196	3.542	+	1102	√	ND	ND
TDP 23	419.1118	420.1196	3.428	+	142685	ND	√	ND
TDP 24	421.1273	422.1339/420.1191	3.831	+/-[d]	186586	√	ND	ND
TDP 25	433.0650	434.0714	3.526	+	20044	√	ND	ND
TDP 26	443.1086	444.1154	3.809	+	15273	√	ND	ND
TDP 27	447.1543	448.1601	3.527	+	15540	√	ND	ND
TDP 28	457.0887	456.0813	3.525	-	33112	√	ND	ND
TDP 29	479.1795	480.1860	3.836	+	13387	√	ND	ND
TDP 30	681.3000	682.3039	3.801	+	162306	ND	√	ND
TDP 31	246.0641	247.0719	3.624	+	7800	ND	ND	√
TDP 32	306.0866	307.0931	3.175	+	11883	ND	ND	√

[a] TDP 22 was not detected in $nSiO_2$–AZOX water model. The other peaks were detected in all three formulations (conventional, Allosperse® and $nSiO_2$)

[b] ESI: Electrospray ionization

[c] Peak area: ESI+ average signal for all treatments

[d]This TDP could be ionized and detected in both negative and positive ESI modes. The respective *m/z* in each mode are indicated.
*The thermal degradation products were only detected in the samples treated with pesticides and were not present in either unheated samples nor heated control samples.

Table 3 List of thermal degradation products (TDPs) tentatively identified (based on PCDL[a] library and MS/MS[b] spectra) in the water (10 µg/mL) and/or the spiked strawberries (1 µg/mg) and/or the incurred strawberries (around 10 µg/kg) after heating 4 hours at 100°C.

Compound[c] (Manufacturer code[d])	ID in this study	Model	Formula	Neutral mass	RT	Precursor ions (*m/z*) ESI+	Main fragment ions (*m/z*) ESI+	Reference
Azoxystrobin	-	water, spiked and incurred strawberry	$C_{22}H_{17}N_3O_5$	403.1169	3.738	404.12467	372.0983	37
Azoxystrobin compound 2 (R234886)	TDP 19	water	$C_{21}H_{15}N_3O_5$	389.1012	3.499	390.10902	372.0981	34
Azoxystrobin compound 3 (R219277)	TDP 6	water and spiked strawberry	$C_{15}H_{14}N_2O_5$	302.0903	2.675	303.09813	-	39
Azoxystrobin compound 18 (R176586)	TDP 1	spiked strawberry	$C_{11}H_{12}O_4$	208.0734	2.906	209.0814	-	33
Azoxystrobin compound 20 (R402173)	TDP 12	water	$C_{19}H_{13}N_3O_4$	347.0906	3.469	348.09845	-	33
Azoxystrobin compound 21	TDP 15	water	$C_{20}H_{15}N_3O_4$	361.1073	3.783	362.1141	-	38
Azoxystrobin compound 26 (R401487)	TDP 31	incurred strawberry	$C_{12}H_{10}N_2O_4$	246.0641	3.624	247.0719	-	33
Azoxystrobin compound 28 (R401553)	TDP 2	water and spiked strawberry	$C_{11}H_7N_3O_2$	213.0538	2.44	214.0617	-	38
Azoxystrobin compound 36 (R403314)	TDP 22	water	$C_{21}H_{17}N_3O_6$	407.1118	3.542	408.11959	348.0982	34,37,38
Azoxystrobin compound New M4	TDP 32	incurred strawberry	$C_{14}H_{14}N_2O_6$	306.0866	3.175	307.0931	-	34

Compound[c] (Manufacturer code[d])	ID in this study	Model	Formula	Neutral mass	RT	Precursor ions (*m/z*) ESI+	Main fragment ions (*m/z*) ESI+	Reference
Azoxystrobin compound 22	TDP 23	spiked strawberry	$C_{22}H_{17}N_3O_6$	419.1118	3.428	420.1196	-	33, 34
Azoxystrobin compound 23								33, 34
Azoxystrobin compound U13							-	33

[a] PCDL: A metabolite library made by Agilent Masshunter PCDL software

[b] MS/MS: Tandem mass spectrometry

[c] The compound: number and letters were commonly used in the literature, except the "new M4", which is found in the study of Gautam, Etzerodt & Fomsgaard[34].

[d] Manufacturer codes of azoxystrobin metabolites were usually used as compounds ID in the literature.

3.3.1 Thermal degradation products in heated water

LC/MS total ion chromatograms (TICs) were obtained in full scan mode (50-750 *m/z*) for all formulations (conventional, Allosperse and $nSiO_2$). As an example, the TICs for AZOX in the $nSiO_2$ formulation (water, 10 µg/mL) before and after heating (100°C, 4 hours) are compared in Figure 3. As expected, the peak corresponding to AZOX decreased after 4 hours of heating. Several relatively large new peaks were observed after heating in both positive (Figure 3a) and negative modes (Figure 3b). These peaks were TDP 7, 11 and 19 (*neutral mass* 303.101, 329.0802 and 389.1012, respectively), which could be detected in both ESI- and ESI+ modes. The MS/MS spectra in ESI+ mode for the three TDPs were showed in Figure S1.

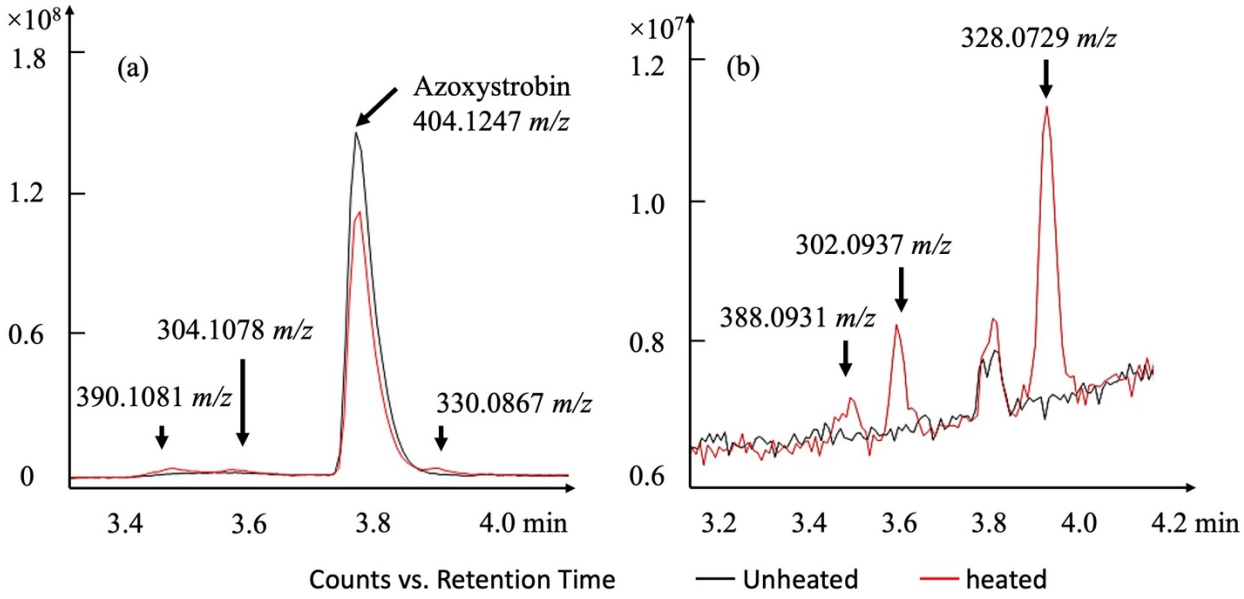

Figure 3 Total Ion Chromatograms (overlap) of the azoxystrobin in $nSiO_2$ formulation in water (10 µg/mL) before and after heating for 4 hours (a: ESI+ and b: ESI-).

Beside the major degradation products of AZOX in water presented in Figure 3, minor degradation products, not directly visible in TICs are listed in Table 2. A total of 23 suspected TDPs were detected in the water. All these suspected TDPs, except TDP 22, were detected in all

of the pesticide formulations (conventional, Allosperse® and $nSiO_2$) samples. The absence of TDP 22 in $nSiO_2$ samples might have been caused by the low levels of TDP 22 in the formulations, especially for the $nSiO_2$ samples, which were below the instrument detection limit. Based on the available information, the heating of nanoencapsulated AZOX did not generate new compounds compared to the conventional formulation. Moreover, six compounds (TDPs 2, 6, 12, 15, 19 and 22) in this study could be matched with substances reported the literature (Table 3). However, 17 other TDPs in water could not be identified due to a lack of information in the literature.

The MS/MS spectra of TDPs 19 and 22 published in the literature were matched with spectra obtained in this study (Table 3), with a second ion (372.0981 *m/z*) observed for AZOX TDP 19. Based on the RT (3.5 min) and MS/MS spectrum of the reference standard of AzFA, TDP 19 was confirmed to be AzFA. AzFA is a major degradation product of AZOX in the environment[40]. As it is known to be toxic to aquatic life, AzFA has been recommended for regulation in water in Denmark[41]. A fragment at 348.0982 *m/z* was recorded for TDP 22, matching with the information of R403314 reported in previous studies on the photochemical transformation of AZOX in water[34,37,38].

3.3.2 Thermal degradation products in the spiked strawberries

In heated spiked strawberries, nine possible TDPs (1-6, 20, 23 and 30) were detected (Table 2). Except for TDP 4, the other TDPs in spiked strawberry model were detected in ESI+ mode. Only two TDPs (2 and 6) were detected in both the water and spiked strawberries. For the target screening with the in-house PCDL library, four TDPs (1, 2, 6 and 23) were tentatively matched with the literature in the spiked strawberry model. Given that three degradation products of AZOX

share the same formula $C_{22}H_{17}N_3O_6$, and since the literature MS/MS data were not available, the tentative identification of TDP 23 (*neutral mass* 419.1118) could not be further confirmed.

Some TDPs had a higher molar mass than the AZOX parent compound (*neutral mass* 403.388), indicating possible reactions with matrices or other TDPs. The reactions of AZOX in water were simpler than in the food matrices, which contain sugars, protein, etc. In environmental samples, AZOX and relevant metabolites had been found conjugated with endogenous molecules such as glucose or carboxylic or amino acids[37]. For example, TDP 2 could react with glucose to form glucosyl-2-{2-[6-(2-cyanophenoxy)pyrimidin-4-yloxy]phenyl}-3-methoxyacrylate in a plant[33]. Thus, AZOX could generate more complex TDPs in food compared to the water model.

3.3.3 Thermal degradation products in the heated incurred strawberries

It is important to first indicate that some degradation products of AZOX may have occured in incurred strawberries prior to thermal processing due to the metabolism or natural degradation of AZOX in the field and during storage. In the present study, once the compounds in the unheated samples were eliminated, there were no additional molecular features of interest in the heated incurred strawberries. Nonetheless, from the target screening with the PCDL library, two compounds (TDPs 31 and 32; Table 3) were detected in heated incurred strawberries, which were not detected in the heated control strawberry. The presence of TDP 31 and 32 may reflect some metabolism and natural degradation of AZOX in the field cultures or during storage. Although TDP 31 could be detected in both unheated and heated incurred strawberries, the peak intensity of TDP 31 in heated samples was higher than in the unheated samples, indicating the thermal degradation of AZOX to form TDP 31. TDP 31 and 32 were not detected in the water or spiked strawberry samples, which further supports the hypothesis that they could be from metabolism or

natural degradation in the field or during storage. All TDPs were detected across all pesticide formulations (conventional, Allosperse® and $nSiO_2$). Therefore, the nanoencapsulation of AZOX did not appear to generate new TDPs in spiked and incurred strawberry models as compared to the conventional formulation.

3.4 Potential degradation pathways of azoxystrobin in water

High temperatures generally accelerate the decomposition of pesticides caused by their hydrolytic degradation in water[35]. According to the tentatively identified TDPs in the previous sections, thermal degradation pathways could be proposed for AZOX (Figure 4). As the ether bond is unstable with heat due to a pair of lone electons on the oxygen atom, it was prone to breakage[42]. The cleavage of the ether linkages between the pyrimidinyl ring to the phenylacrylate ring and to the cyanophenyl ring of AZOX is proposed to generate TDPs 2 and 6, respectively. Oxidative o-dealkylation of AZOX could produce TDP 19, which was identified as AzFA. From the intensity of molecular ion peak in Figure 3, TDP 19 can be proposed as one of the major thermal products of AZOX. The cyano group (-C≡N) on the benzene ring of TDP 19 could be hydrolyzed, leading to some rearrangement reactions[43]. The cyano group may react with hydrogen ions and water molecules to form a carbon-oxygen double bond (C=O) to give TDP 22. In another pathway, AZOX after demethylation, oxidation and decarboxylation would give AZOX TDP 15[44]. Then TDP 15 could also undergo demethylation to generate TDP 12.

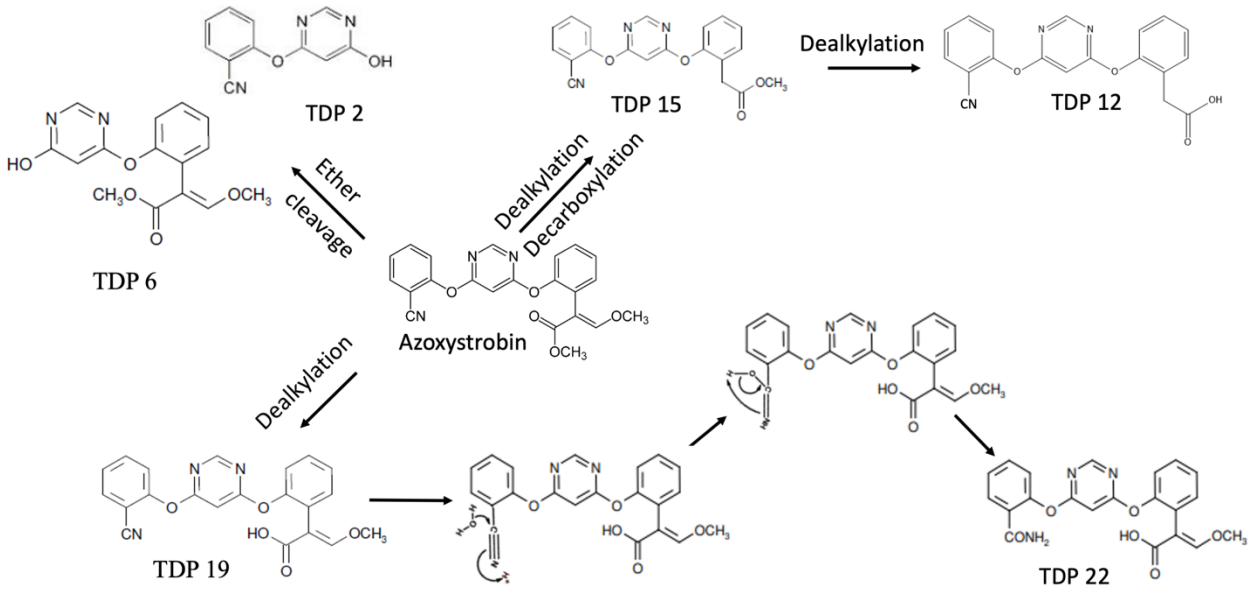

Figure 4 Proposed thermal degradation pathways for azoxystrobin in water following heating for 4 hours.

This present study investigated the thermal degradation of AZOX from simple matrices to more complex matrices, and from laboratory control samples to 'real' samples. This study contributes to reduce the knowledge gaps related to AZOX dissipation in food[45]. AZOX degradation for both the conventional and nanoencapsulated formulations followed first-order kinetics when heated at 100°C in the water. Different TDPs were identified in water, spiked and incurred strawberries. To the best of our knowledge, this is the first report on the TDPs of AZOX (conventional and nanoencapsulated formulations) for both water and food models. This study highlighted some knowledge gaps in our understanding of the degradation products of pesticides in the environment and during food processing. Many TDPs in water have not been reported in the literature, even some TDPs of AZOX with relatively high intensity (e.g. TDPs 7 and 11, Figure 3). Toxicity studies usually focus on the parent azoxystrobin compound, and little toxicological information is available for its metabolites[46]. Therefore, further identification and toxicity studies

of the unknown degradation products are necessary to fully assess the health risk which may be associated with the degradation products of AZOX.

Overall, nanocarriers had a slight or no impact either on the degradation rate or on the degradation product types, and there was no evidence that this could change the thermal degradation pathways of AZOX. Nonetheless, we must be very careful about the introduction of new nanotechnologies into our food chain. It is possible unforeseeable associated risks to human health and environment, which may accompany its positive potential.

5. Supporting information

A description of the pesticide treatments, the synthesis approach for nanoencapsulated AZOX pesticides, quality assurance/quality control data, MS/MS spectra for some TDPs, and a list of AZOX metabolites and degradation products.

6. Acknowledgements

We wish to acknowledge the Vive Crop Protection Inc. for providing the pesticide formulations. We thank Michael Bleho, Laura Caralampides and the team at the Hort Center for the support with the field experiment.

7. Funding sources

This research was funded in part by the Natural Sciences and Engineering Research Council of Canada (grant nos. RGPIN-2016-05022, STPGP 506450-17) and the Fonds de Recherche du Québec - Nature et Technologies (FRQNT, grant no. 286120). We wish to acknowledge the financial support from the Canada Foundation for Innovation/John R. Evans

Leaders Fund grant (Project #35318) research grants to SB. V.B. was supported in part by a McGill Engineering Doctoral Award. J.A.G. was supported by FRQNT (grant no. 255500). P.W. was supported by a Pylarcyk scholarship.

References

1. Yigit, N., & Velioglu, Y. S. (2020). Effects of processing and storage on pesticide residues in foods. *Crit. Rev. Food Sci. Nutr.*, *60*(21), 3622-3641.
2. Li, C., Zhu, H., Li, C., Qian, H., Yao, W., & Guo, Y. (2021). The present situation of pesticide residues in China and their removal and transformation during food processing. *Food Chem.*, *354*, 129552.
3. Lan, J., Sun, W., Chen, L., Zhou, H., Fan, Y., Diao, X., Wang, B., & Zhao, H. (2020). Simultaneous and rapid detection of carbofuran and 3-hydroxy-carbofuran in water samples and pesticide preparations using lateral-flow immunochromatographic assay. *Food Agric. Immunol.*, *31*(1), 165-175.
4. Codex Alimentarius. (2010). Codex general standard for contaminants and toxins in food and feed (CODEX STAN 193–1995).
5. Zobir, S. A. M., Ali, A., Adzmi, F., Sulaiman, M. R., & Ahmad, K. (2021). A review on nanopesticides for plant protection synthesized using the supramolecular chemistry of layered hydroxide hosts. *Biology*, *10*(11), 1077.
6. Ruiz-Romero, P., Valdez-Salas, B., González-Mendoza, D., & Mendez-Trujillo, V. (2018). Antifungal effects of silver phytonanoparticles from Yucca shilerifera against strawberry soil-borne pathogens: Fusarium solani and Macrophomina phaseolina. *Mycobiology*, *46*(1), 47-51.
7. Rebollar, A., Madden, L., & Ellis, M. (2007). Pre-and post-infection activity of azoxystrobin, pyraclostrobin, mefenoxam, and phosphite against leather rot of strawberry, caused by *Phytophthora cactorum*. *Plant Dis.*, *91*(5), 559-564.

8. Carisse, O., Lefebvre, A., Van der Heyden, H., Roberge, L., & Brodeur, L. (2013). Analysis of incidence–severity relationships for strawberry powdery mildew as influenced by cultivar, cultivar type, and production systems. *Plant Dis., 97*(3), 354-362.
9. Di, S., Wang, Y., Xu, H., Wang, X., Yang, G., Chen, C., Yang, X., & Qian, Y. (2021). Comparison the dissipation behaviors and exposure risk of carbendazim and procymidone in greenhouse strawberries under different application method: Individual and joint applications. *Food Chem., 354*, 129502.
10. Lu, T., Zhang, Q., Lavoie, M., Zhu, Y., Ye, Y., Yang, J., Paerl, H., Qian, H., & Zhu, Y. G. (2019). The fungicide azoxystrobin promotes freshwater cyanobacterial dominance through altering competition. *Microbiome, 7*(1), 1-13.
11. Health Canada, (2016). Proposed Maximum Residue Limit PMRL2016-10, Azoxystrobin. Retrieved December 4, 2021, from https://www.canada.ca/en/health-canada/services/consumer-product-safety/pesticides-pest-management/public/consultations/proposed-maximum-residue-limit/2016/azoxystrobin-2/document.html
12. Balba, H. (2007). Review of strobilurin fungicide chemicals. *J. Environ. Sci. Health., Part B, 42*(4), 441-451.
13. Galhardi, J. A., Wang, P., Bueno, V., Ghoshal, S., Gravel, V., Wilkinson, K. J., & Bayen, S. (2022). Field evaluation of the potential effects of polymer and silica-based nanopesticides on strawberries and agricultural soils. *Environ. Sci.: Nano.* Accepted.
14. Pandey, V., Sharma, R.M., Yamdagni, R., Dubey, A.K. & Jadhav., T. U. Introduction. In *Strawberries: Production, Postharvest Management and Protection*; Sharma, R. M., Yamdagni, R., Dubey, A. K., Pandey, V. Eds.; CRC Press: Pkwy, NW, 2019; pp.1-16.

15. Gavahian, M., Pallares, N., Al Khawli, F., Ferrer, E., & Barba, F. J. (2020). Recent advances in the application of innovative food processing technologies for mycotoxins and pesticide reduction in foods. *Trends Food Sci. Technol.*, *106*, 209-218.
16. Hou, F., Teng, P., Liu, F., & Wang, W. (2017). Tebuconazole and azoxystrobin residue behaviors and distribution in field and cooked peanut. *J. Agric. Food Chem.*, *65*(22), 4484-4492.
17. Aguilera, A., Valverde, A., Camacho, F., Boulaid, M., & Garcia-Fuentes, L. (2012). Effect of household processing and unit to unit variability of azoxystrobin, acrinathrin and kresoxim methyl residues in zucchini. *Food Control*, *25*(2), 594-600.
18. Lozowicka, B., & Jankowska, M. (2016). Comparison of the effects of water and thermal processing on pesticide removal in selected fruit and vegetables. *J. Elem.*, *21*(1).
19. Yang, A., Park, J., Abd El-Aty, A., Choi, J., Oh, J., Do, J., Kwon, K., Shim, K., Choi, O., & Shim, J. H. (2012). Synergistic effect of washing and cooking on the removal of multi-classes of pesticides from various food samples. *Food Control*, *28*(1), 99-105.
20. Jiang, Y., Shibamoto, T., Li, Y., & Pan, C. (2013). Effect of household and commercial processing on acetamiprid, azoxystrobin and methidathion residues during crude rapeseed oil production. *Food Addit. Contam., Part A*, *30*(7), 1279-1286.
21. Peng, W., Zhao, L., Liu, F., Xue, J., Li, H., & Shi, K. (2014). Effect of paste processing on residue levels of imidacloprid, pyraclostrobin, azoxystrobin and fipronil in winter jujube. *Food Addit. Contam., Part A*, *31*(9), 1562-1567.
22. Jankowska, M., Kaczynski, P., Hrynko, I., & Lozowicka, B. (2016). Dissipation of six fungicides in greenhouse-grown tomatoes with processing and health risk. *Environ. Sci. Pollut. Res.*, *23*(12), 11885-11900.

23. Li, S., Sun, M., Wang, F., Xu, X., Zhang, X., Ma, J., Xiao, J., Liao, M., & Cao, H. (2019). Dissipation behavior of three fungicides during the industrial processing of Paeoniae Radix Alba and associated processing factors. *Int. J. Environ. Res. Public Health*, *16*(12), 2196.
24. Jankowska, M., Lozowicka, B., & Kaczynski, P. (2019). Comprehensive toxicological study over 160 processing factors of pesticides in selected fruit and vegetables after water, mechanical and thermal processing treatments and their application to human health risk assessment. *Sci. Total Environ.*, *652*, 1156-1167.
25. Tian, L., & Bayen, S. (2018). Thermal degradation of chloramphenicol in model solutions, spiked tissues and incurred samples. *Food chem.*, *248*, 230-237.
26. Baesu, A., Audet, C., & Bayen, S. (2021). Application of non-target analysis to study the thermal transformation of malachite and leucomalachite green in brook trout and shrimp. *Curr. Res. Food Sci.*, *4*, 707-715.
27. Organisation for Economic Co-operation and Development (OECD) (2008). OECD Guideline for the testing of chemicals 508: magnitude of the pesticide residues in processed commodities.
28. Bueno, V., & Ghoshal, S. (2020). Self-Assembled Surfactant-Templated Synthesis of Porous Hollow Silica Nanoparticles: Mechanism of Formation and Feasibility of Post-Synthesis Nanoencapsulation. *Langmuir*, *36*(48), 14633-14643.
29. Bueno, V., Wang, P., Harrisson, O., Bayen, S., & Ghoshal, S. (2022). Impacts of a Porous Hollow Silica Nanoparticle-Encapsulated Pesticide Applied to Soils on Plant Growth and Soil Microbial Community. *Environ. Sci.: Nano.*, *9*, 1476-88.
30. Lehotay, S. (2007). AOAC official method 2007.01 pesticide residues in foods by acetonitrile extraction and partitioning with Magnesium Sulfate. *J. AOAC Int.*, *90*(2), 485-520.

31. Wang, P., Galhardi, J. A., Liu, L., Bueno, V., Ghoshal, S., Gravel, V., Wilkinson, K. J. & Bayen, S. (2022). Development of an LC-MS-based method to study the fate of nanoencapsulated pesticides in soils and strawberry plant. *Talanta*, 123093.
32. Tian, L., Khalil, S., & Bayen, S. (2017). Effect of thermal treatments on the degradation of antibiotic residues in food. *Crit. Rev. Food Sci. Nutr.*, *57*(17), 3760-3770.
33. FAO (2009). AZOXYSTROBIN (229) in pesticide residues in food 2008. Plant production and protection paper 193:55. Retrieved November 11, 2021, from: http://www.fao.org/fileadmin/templates/agphome/documents/Pests_Pesticides/JMPR/Evaluation08/Azoxystrobin.pdf.
34. Gautam, M., Etzerodt, T., & Fomsgaard, I. S. (2017). Quantification of azoxystrobin and identification of two novel metabolites in lettuce via liquid chromatography–quadrupole-linear ion trap (QTRAP) mass spectrometry. *Int. J. Environ. Anal. Chem.*, *97*(5), 419-430.
35. Khandelwal, A., Gupta, S., Gajbhiye, V. T., & Varghese, E. (2016). Degradation of Kresoxim-Methyl in Water: Impact of Varying pH, Temperature, Light and Atmospheric CO 2 Level. *Bull. Environ. Contam. Toxicol.*, *96*(1), 130-136.
36. Chariou, P. L., Ortega-Rivera, O. A., & Steinmetz, N. F. (2020). Nanocarriers for the delivery of medical, veterinary, and agricultural active ingredients. *ACS nano*, *14*(3), 2678-2701.
37. Bauer, A., Luetjohann, J., Hanschen, F. S., Schreiner, M., Kuballa, J., Jantzen, E., & Rohn, S. (2018). Identification and characterization of pesticide metabolites in Brassica species by liquid chromatography travelling wave ion mobility quadrupole time-of-flight mass spectrometry (UPLC-TWIMS-QTOF-MS). *Food Chem.*, *244*, 292-303.

38. Boudina, A., Emmelin, C., Baaliouamer, A., Paisse, O., & Chovelon, J. M. (2007). Photochemical transformation of azoxystrobin in aqueous solutions. *Chemosphere*, *68*(7), 1280-1288.
39. Singh, N., Singh, S. B., Mukerjee, I., Gupta, S., Gajbhiye, V. T., Sharma, P. K., Goel, M., & Dureja, P. (2010). Metabolism of ^{14}C-azoxystrobin in water at different pH. *J. Environ. Sci. Health., Part B*, *45*(2), 123-127.
40. Gautam, M., & Fomsgaard, I. S. (2017). Liquid chromatography-tandem mass spectrometry method for simultaneous quantification of azoxystrobin and its metabolites, azoxystrobin free acid and 2-hydroxybenzonitrile, in greenhouse-grown lettuce. *Food Addit. Contam., Part A*, *34*(12), 2173-2180.
41. Jorgensen, L. F., Kjaer, J., Olsen, P., & Rosenbom, A. E. (2012). Leaching of azoxystrobin and its degradation product R234886 from Danish agricultural field sites. *Chemosphere*, *88*(5), 554-562.
42. Hu, J., Shen, D., Wu, S., Zhang, H., & Xiao, R. (2015). Catalytic cleavage of C–O linkages in benzyl phenyl ether assisted by microwave heating. *RSC Adv.*, *5*(55), 43972-43977.
43. Chen, F., Yang, D., Yu, F., Kun, Y., & Song, Y. (2021). The Effect of Mass Transfer Rate-Time in Bubbles on Removal of Azoxystrobin in Water by Micro-Sized Jet Array Discharge. *Catalysts*, *11*(10), 1169.
44. Feng, Y., Huang, Y., Zhan, H., Bhatt, P., & Chen, S. (2020). An overview of strobilurin fungicide degradation: Current status and future perspective. *Front. Microbiol.*, *11*, 389.
45. Bian, Y., Guo, G., Liu, F., Chen, X., Wang, Z., & Hou, T. (2020). Meptyldinocap and azoxystrobin residue behaviors in different ecosystems under open field conditions and distribution on processed cucumber. *J. Sci. Food Agric.*, *100*(2), 648-655.

46. Rodrigues, E., Lopes, I., & Pardal, M. (2013). Occurrence, fate and effects of azoxystrobin in aquatic ecosystems: a review. *Environ. Int., 53*, 18-28.